EUROFUSION WPMST1-PR(16) 14781

D Carralero et al.

A study on the density shoulder formation of H-mode plasmas

Preprint of Paper to be submitted for publication in
22nd International Conference on Plasma Surface Interactions
in Controlled Fusion Devices (22nd PSI)

This work has been carried out within the framework of the EUROfusion Consortium and has received funding from the Euratom research and training programme 2014-2018 under grant agreement No 633053. The views and opinions expressed herein do not necessarily reflect those of the European Commission.

A study on the H-mode density shoulder formation

D. Carralero[a*], J. Madsen[b], S. A. Artene[a,c], M. Bernert[a], G. Birkenmeier[a,c], T. Eich[a], G. Fuchert[d], F. Laggner[a], V. Naulin[b], P. Manz[c], N. Vianello[e,f], E. Wolfrum[a], the EUROfusion MST1 team[g] and the ASDEX Upgrade Team[a].

[a] *Max Planck Institute for Plasma Physics, Boltzmannstr. 2, 85748 Garching, Germany* [b] *Aalto University, Espoo, Finland.*[c]*Physik-Department E28, Technische Universität München, Garching, Germany.*[d] *Max Planck Institute for Plasma Physics, Greifswald, Germany.*[e]*Consorzio RFX, Padova, Italy* [f]*Ecole Polytechnique Fédérale de Lausanne, Swiss Plasma Center (SPC), Lausanne, Switzerland* [g]*See http://www.euro-fusionscipub.org/mst1*

Abstract

The shoulder formation is an increase of the decay length of the scrape-off layer (SOL) observed in many tokamaks during L-mode operation when a density threshold is reached. Recent experiments in ASDEX Upgrade (AUG) and JET have shown how shoulder formation occurs when divertor collisionality disconnects filaments from the wall. This leads to a transition from sheath limited to inertial regime filaments and to the enhancement of perpendicular transport, in good agreement with analytical models. In the present work, the validity of such shoulder formation mechanism is investigated in the more reactor-relevant H-mode. For this, a cold divertor H-mode scenario is developed in AUG using different levels of D puffing and N seeding, in which inter-ELM filaments and SOL density profiles are measured. The basic relation between filament size and divertor collisionality is still valid in H-mode plasmas, albeit a new condition related to D puffing has been found for the formation of the shoulder.

PACS: 52.55.-s, 52.55.Fa, 52.35.Ra, 52.55.Rk
PSI-20 keywords: ASDEX-Upgrade, Detachment, Edge plasma, Intermittent transport, H-mode

**Presenting/corresponding author address*: Boltzmannstrasse, 2 D-85748 Garching, Germany.

**Presenting/corresponding author E-mail*: daniel.carralero@ipp.mpg.de

1. Introduction

The next generation of magnetic confinement fusion devices will need to solve the problem of heat and particle fluxes on Plasma-Facing Components (PFC), which will almost certainly stretch available materials to their technical limits on power loads and erosion levels [1]. In particular, the prediction of particle and heat fluxes into the main will require the development of a working model for perpendicular transport in the far Scrape-off Layer (SOL), including the propagation of filamentary structures [2]. Recent work carried out in ASDEX Upgrade (AUG) [3] advanced in this direction by confirming experimentally the predictions of filament propagation analytical models [4-6], which explained the broadening of L-mode SOL density profiles observed in many tokamaks (sometimes referred to as "shoulder") [7,8] in terms of a filament regime transition. In it, it was shown how the parameter regulating shoulder formation is the effective collisionality parameter from [6] defined in the divertor region, Λ_{div}. When this parameter, representing the product of characteristic parallel transport time and ion-electron collision frequency, becomes $\Lambda_{div} > 1$, filaments are electrically disconnected from the wall, thus transitioning from the sheath limited to the inertial regime and greatly enhancing the perpendicular transport.

According to these findings, baseline scenarios of ITER and DEMO would feature fully developed shoulders, as the estimated values of Λ_{div} will greatly exceed that threshold [9]. This could be of great practical importance, since it could substantially increase the particle flux arriving to the first wall, as well as contribute to spread particle and power fluxes on the divertor target. Both effects would have relevant consequences on the sputtering yield of the PFCs of both regions, thus changing the predicted life times of several components. However, the regime transition model has only been tested in L-mode plasmas, while next generation devices will operate in H-mode. Therefore, before these predictions can be considered, it is necessary to prove that shoulder formation does also happen in H-mode, and if so, that the same mechanism found in

L-mode applies. Regarding the first question, several examples of an H-mode shoulder formation can be found in the literature [10, 11], but no systematic study has been realized so far. Besides, this problem must be separated from ELM-related transport, which usually dominates the SOL of present day machines operating in H-mode, as ITER and especially DEMO will feature substantially reduced levels of ELM activity [12]. In the present work, we present the results of a series of experiments carried out in AUG with the aim of inducing a shoulder formation during inter-ELM H-mode periods and validating the filament transition model by measuring the evolution of filaments and Λ_{div} during the process.

2. Experiments

In order to evaluate the filament transition model, the evolution of filament characteristics and SOL density profiles was to be measured while Λ_{div} was varied across the L-mode threshold (Λ_{div} ϵ [0.1, 10]) in a constant density H-mode plasma. Thus, a new scenario was developed using the same magnetic geometry (LSND edge optimized configuration) and plasma parameters (B_T = 2.5 T, I_p = 800 kA, q_{95} = 4.85) as in L-mode discharges used in previous work [3]. In it, sufficient ECH and NBI power was added to access H-mode, while keeping total heating low enough to allow midplane manipulator (MPM) measurements in the SOL (See Table 1). Given this limitation, this scenario was far from H-mode LFS divertor detachment and Nitrogen seeding was required to obtain a cold, collisional divertor. In order to disentangle the effects of Nitrogen and Deuterium puff on Λ_{div} values, different sets of values of each (N_{rate} and D_{rate}) were used, roughly dividing the data set in four scenarios: A) low power discharges with low N_{rate} and D_{rate} values; B) discharges including both NBI and ECH heating, strong Nitrogen seeding and low to moderate N_{rate}; C) A discharge in which $\Lambda_{div} > 1$ is achieved only by means of a strong D_{rate}; D) discharges with full power, and both high N_{rate} and D_{rate} values.

A typical discharge is presented in Figure 1: in it, three main phases can be distinguished: first, only 300 kW of heating are used to establish a reference L-mode. Next, full power is injected and H-mode with type-I ELMs is accessed. Finally, the Λ_{div} scan is carried out by increasing N_{rate} and/or D_{rate}. This ends the type-I ELMs and replaces them with smaller, more frequent ones. Also, the divertor temperature is reduced, bringing the LFS divertor to several levels of detachment. During the whole discharge, divertor conditions and midplane density profiles are measured, respectively, by the set of divertor fixed Langmuir probes [13] and the Lithium Beam [14]. Λ_{div} is calculated as explained in [3], using divertor target values of n_e and T_e and a fraction of $\pi R q_{95}$ as the characteristic parallel length. Additionally, the MPM is equipped with the 14-pin probe head used in L-mode experiments, providing the perpendicular size and velocity of filaments by correlating ion saturation measurements in poloidaly and radially spaced pins [15]. As can be seen in Figure 1, the MPM is plunged multiple times during the discharge, covering each phase, and several values of Λ_{div}.

3. Analysis and Results

3.1 ELM Conditional Averaging

In these H-mode plasmas, ELMs introduce a new level of complexity in the analysis of data: in L-mode, fluctuations do not substantially alter the background conditions of the SOL, and both divertor conditions and midplane density profiles can be measured separately. However, the ejection of ELMs in H-mode creates a major and intermittent perturbation across the whole SOL. Therefore, the ELM cycle has to be taken into account when defining the turbulent characteristics of transport. With this aim, the H-mode phase of each discharge is divided in 250 ms windows and ELMs are detected using the thermoelectric currents to the divertor, I_{div} [16]. Then, divertor Langmuir probes and Lithium beam measurements during each ELM are used to obtain an

average evolution of Λ_{div} and midplane n_e profiles as a function of $t\text{-}t_{E,max}$, where $t_{E,max}$ is the time of the maximum I_{div} value. Finally, for each window, pre-ELM phase ($t\text{-}t_{E,max}$ = -2 ms) density and collisionality values are taken, as being representative of inter-ELM conditions [17]. This method is not valid for MPM data, as the conditional analysis must be performed around fluctuations and only the limited intervals in which the manipulator is inserted are available. In this case, I_{div} is used to separate "inter-ELM" probe data from "close to an ELM" data (ie., 3ms > $t\text{-}t_{E,max}$ > -2 ms). Then, only the first group is considered, and filament conditional analysis is performed using a 2.5σ threshold, as in previous work [15].

3.2 Shoulder formation

According to L-mode theory, in those discharges in which the D_{rate} and/or N_{rate} are high enough to achieve $\Lambda_{div} > 1$, a shoulder formation should be observed by the end of the third phase (high collisionality H-mode). In Fig. 2, some inter-ELM density profiles are presented at the beginning of the H-mode (t = 3.75 s, dashed line) and at the end of the third phase (t = 6 s, solid line). As can be seen, some of them (33056, 33059) exhibit a clear flattening at the end of the discharge, while in the other two little or no flattening can be seen in the same interval. In order to quantify this effect, two e-folding lengths are defined on the profile: First, $\lambda_{n,far}$, representing the evolution of the profile in the far SOL, is fitted in the $\rho_p \in [1, 1.04]$ radial range. This parameter is equivalent to the λ_n used in previous work to detect the shoulder formation [3, 15]. Second, $\lambda_{n,sep}$, representing the evolution around the separatrix, is fitted in the $\rho_p \in [0.98, 1.01]$ range. Also, Λ_{div} is calculated using the fixed probes in the $\rho_p \in [1.02, 1.04]$ range. In Figure 2, the evolution of Λ_{div} through the discharge is represented as a function of D_{rate} to show the different trends obtained in the four scenarios described in Section 2. The same color code is used as in Table 1 (respectively, light blue/dark blue/black/reddish for scenarios A-D). As can be seen, only

scenarios with high N_{rate} surpass clearly the $\Lambda_{div} > 1$ threshold. Instead, the low N_{rate}, low D_{rate} scenario remains clearly under the threshold, and the one with $N_{rate} = 0$, slightly over it by the end of the discharge. The differences between the four scenarios can be seen in the right plot of figure 2, where the relation between inter-ELM Λ_{div} and $\lambda_{n,far}$ is represented using the same color code over a shaded background representing the trend found in L-mode experiments. Considering the point cluster as a whole, a behavior similar to that of L-mode is found, with $\lambda_{n,far}$ raising after $\Lambda_{div} >1$, even if the increase is not as sharp and the $\lambda_{n,far}$ values are not as high. However, when the four scenarios are considered, a clearer trend is found: discharges from scenario A display low levels of Λ_{div} and do not access the higher transport regime. The same is valid essentially for scenario C, albeit slightly higher Λ_{div} (and thus $\lambda_{n,far}$) values are achieved. Instead, all discharges from scenario D develop a clear shoulder, achieving a significant increase in $\lambda_{n,far}$ at higher values of Λ_{div}. Interestingly, discharges in scenario B, displaying similar Λ_{div} values as those in scenario D, fail to achieve high $\lambda_{n,far}$ values.

3.3 Filament Characteristics

The main results of conditional analysis on MPM data are shown in figure 3: the evolution of filament size with edge line-integrated density shows two thresholds after which the size increases sharply: the first one is around $N_{edge} > 2 \cdot 10^{19}$ m^{-3}, and coincides with the L-mode shoulder formation detected previously for 300 kW operation [3]. The second is around $N_{edge} > 3.75 \cdot 10^{19}$ m^{-3}, and would correspond to an equivalent threshold for H-mode. Instead, when the same data points are represented as a function of Λ_{div}, the two thresholds merge around $\Lambda_{div} > 1$, in good agreement with the filament regime transition hypothesis, and suggesting that the same disconnection mechanism applies in H-mode. Besides that, some properties of filaments change when going from L to H-mode: first, as can be seen in figure 3, pre-transition filaments tend to be

larger in size in H-mode. Also, the relative amplitude of filaments (expressed as the ratio between the standard deviation and mean values of ion saturation pins, σ/μ) is increased by 30% in H-mode (from $\sigma/\mu \sim 0.35–0.4$ to $\sigma/\mu \sim 0.45–0.55$). This effect is mostly due to the reduction in density in the SOL, and disappears when σ/N_{edge} is used instead. Finally, the detection frequency is reduced for $\Lambda_{div} < 1$, with typical values in the range of $f_d \in [2000,2500]$ s^{-1} and $f_d \in [1000,1500]$ s^{-1} for L and H-mode, respectively.

3.4 Near SOL evolution

Besides the evolution of $\lambda_{n,far}$, the relation of the density gradient at the separatrix with the process of shoulder formation has been observed: By comparing $\lambda_{n,far}$ and $\lambda_{n,sep}$ in the dataset, it could be concluded that no correlation exists between then, and thus neither with the Λ_{div} parameter responsible for shoulder formation. Instead, as shown in figure 4, $\lambda_{n,sep}$ could be correlated to other parameters: First, there seems to be a clear correlation between D_{rate} and $\lambda_{n,sep,}$ both in discharges with constant and variable levels of the former (no such relation is found between N_{rate} and $\lambda_{n,sep}$, though). Second, ELM frequency is proportional to the $\lambda_{n,sep}$ value.

4. Discussion and Conclusions

The first conclusion coming from the data could be that a phenomenon analogous to the well documented L-mode shoulder formation can be found when a density threshold is surpassed under certain conditions in inter-ELM periods of H-mode: indeed, as seen in figure 5, some of the discharges have a sharp increase in $\lambda_{n,far}$ for $N_{edge} > 3.7\ 10^{-19}$ m^{-3}. As well, the role of Λ_{div} as the parameter regulating the formation of the shoulder seems to be also generally valid in H-mode: as can be seen, only discharges with $\Lambda_{div} > 1$ in figure 2 (namely those in scenario D) display a clear shoulder over the density threshold. However, this study reveals a more complex picture as in L-mode, as the $\Lambda_{div} > 1$ seems to be necessary but not sufficient for the shoulder formation: shots in

scenario B do not reach high levels of $\lambda_{n,far}$ despite having high collisionality in the divertor. As the data in figure 2 reveal, this happens for discharges with low D_{rate}, indicating the existence of a second threshold for the shoulder, related to the gas puffing level. One possible explanation for this would be that the shoulder formation requires a high recycling regime rate in the main wall on top of the increased convective transport [18]. This would be in good agreement with recent experiments which show how far-SOL ion temperatures drop after the shoulder formation [19,20], suggesting that a large fraction of the ions in it do not come from the confined plasma but from ionization of recycled neutrals. In such case, a minimum level of neutral density in the far SOL could be required to start the process, thus requiring a minimum value of D_{rate}. The precise determination of this second threshold and the identification of the underlying physical mechanism will be the subject of forthcoming work.

A second conclusion would be that the same regime transition seems to take place as in L-mode, since filament size is substantially increased when high collisionality disconnects the SOL from the wall. Also, the relation between filament transition and shoulder formation seems to hold, as they both share the same Λ_{div} and N_{edge} thresholds. A more direct comparison can be seen in figure 5, where the sizes of filaments measured during some discharges in figure 2 are shown. A general correlation between filament size and $\lambda_{n,far}$ appears, suggesting a relation between increased filamentary transport and the flattening of the profiles. This correlation would also mean that large filaments only appear when a shoulder is formed as discharges in scenario B seem to display smaller sizes than those in scenario D. Unfortunately, the filament and density profile databases do not overlap completely (not all discharges had the MPM equipped with the right probe head, probe data is limited to the reciprocations, etc.), so given the limited amount of data and the large error bars in the filament size calculation, no conclusive statement can be made yet. The clarification of this subject will also be addressed in forthcoming works.

Finally, the density gradient in the separatrix has been found to be largely independent from the collisionality at the divertor, but correlated to D_{rate} and inversely proportional to the ejection frequency of ELMs. This last point would be consistent with previous experiments carried out in AUG [Herrman], which showed how, as the size of ELMs decreases (as seen in figure 1), so does the recovery time of the pedestal (thus increasing their ejection frequency). Nevertheless, the correlation between the ELM cycle and the density gradient can be considered a novel result, as the peeling-ballooning theory associates ELM stability with pressure gradient instead []. Further analysis on this point must be carried out.

Summarizing, the results presented in this work allow the extension of the general shoulder formation mechanism validated in L-mode to H-mode plasmas, introducing a few new elements, such as the influence of the puffing rate. This new understanding of H-mode density transport in the far SOL is a key milestone on the way to a general scaling of the SOL width, capable of improving current predictions for ITER and DEMO operation.

Acknowledgements

This work has been carried out within the framework of the EUROfusion Consortium and has received funding from the Euratom research and training programme 2014-2018 under grant agreement No 633053. The views and opinions expressed herein do not necessarily reflect those of the European Commission.

References

[1] A. Loarte, M. Sugihara, M. Shimada et al., 22nd IAEA Fusion Energy Conference (2008)

[2] S.I. Krasheninnikov 2001 Phys. Lett. A 238 368–70

[3] D. Carralero, P. Manz, L. Aho-Mantila, et al., Phys. Rev. Lett. 115, 215002 (2015)

[4] S.I. Krasheninnikov, D.A. D'Ippolito and J.R. Myra 2008 J. Plasma Phys. 74 679717

[5] J. R. Myra, D. A. Russell, and D. A. D´Ippolito, Phys. Plasmas, 13, 112502 (2006)

[6] O.E. Garcia, R. A. Pitts, J. Horacek, et al J. Nucl. Mater. 363–365 575–80 (2007)

[7] B. LaBombard, R. L. Boivin, M. Greenwald et al., Phys. Plasmas, 8, 2107 (2001)

[8] D.L. Rudakov, J.A. Boedo, R.A. Moyer et al., Nucl. Fusion, 45, 1589-1599 (2005)

[9] D. Carralero, H.W. Müller, M. Groth, et al. J. Nucl. Mater., 463 (2015) 123–127

[10] H. W. Müller , M. Bernert, D. Carralero et al., J. Nucl. Mater., 463, 0 (2015), 739-743

[11] H. J. Sun , E. Wolfrum, T. Eich et al., Plasma Phys. Control. Fusion, 57, 12 (2015), 125011

[12] R.P. Wenninger, M. Bernert, T. Eich, et al. Nucl. Fusion 54 (2014) 114003

[13] M. Weinlich, A. Carlson, Contrib. Plasma Phys. 36 (1996) S, 53-60

[14] M. Willensdorfer, G. Birkenmeier, R. Fischer, et al., Plasma Phys. Control. Fusion, (2014), 56 025008

[15] D. Carralero, G. Birkenmeier, H. W. Müller et al, Nucl. Fusion 54 (2014) 123005

[16] A. Kallenbach, R. Dux, J. C. Fuchs, et al., Plasma Phys. Control. Fusion, 52, 055002 (2010).

[17] A. Burckhart, E. Wolfrum, R. Fischer, et al. Plasma Phys. Control. Fusion, 52, 105010 (2010).

[18] Lipschultz B., Whyte D. and LaBombard B. Plasma Phys. Control. Fusion 47 (2005) 1559–78

[19] D. Carralero, H. J. Sun, S. A. Artene, 42th EPS Conference on Plasma Physics, Lisbon, Portugal (2015)

[20] S. Y. Allan, S. Elmore, G. Fishpool, Plasma Phys. Control. Fusion 58 (2016) 045014

‘

Captions

Figure 1: The three phases on a typical discharge. Top) Edge line integrated density N_{edge} and heating power are shown along with the radial position of the MPM. Middle) Divertor thermoelectric current (indicative of ELM activity), divertor T_e and Λ_{div} in the ρ=1.02-1.04 area of the target. Bottom) Puffing and N seeding rates D_{rate} and N_{rate}.

Figure 2: Experimental results. Left) Several inter-ELM Lithium beam density profiles during the two H-mode phases of the discharge. Separatrix and far SOL e-folding lengths $\lambda_{n,sep}$ and $\lambda_{n,far}$ are indicated. Middle) Parameter diagram, where the collisionality and D_{rate} of each discharge are displayed. Right) Evolution of inter-ELM $\lambda_{n,far}$ with Λ_{div} for the whole set of discharges. The shaded area represents the range of L-mode values shown in [3]. The color code in all plots corresponds to the four scenarios A-D presented in Table 1

Figure 3: Inter-ELM filament size. Left) As a function of line integrated edge density. Right) As a function of Λ_{div}. Shaded area corresponds to L-mode values from [3]. Color indicates L/H-mode.

Figure 4: Inter-ELM separatrix density e-folding length, $\lambda_{n,sep.}$ Left) as a function of puffing rate D_{rate}. Right) As a function of ELM frequency. Color code as in figure 2.

Figure 5: Left) Relation between filament size and $\lambda_{n,far}$. Right) Scaling of $\lambda_{n,far}$ with edge line integrated density, N_{edge}. Same set of discharges and color code as in figure 2.

Table 1: Main parameters of the discharges. The four scenarios A-D are grouped in four colors (respectively, light blue/dark blue/black/reddish), based on their D_{rate}, N_{rate} values.

Tables

Shot	Scenario	P_{ECH} (MW)	P_{NBI} (MW)	$D_{rate\ t=3.5\ s}$ (10^{21} s^{-1})	$N_{rate\ t=4.5\ s}$ (10^{21} s^{-1})	D_{rate} max (10^{21} s^{-1})	N_{rate} max (10^{21} s^{-3})	$T_{e,div}$ min (eV)
31974	**Low N, Low D**	1.3	-	1.33	2.8	1.33	3.4	1
31977		1.9	-	1.33	2.8	1.33	3.8	0
33055	**High N, Low D**	1.34	1.7	6	1.78	6	8	1.5
33057		1.34	1.7	8.19	1.8	8.19	8	3
33056	**High D, no N**	1.34	1.7	6.31	-	24.5	-	10
33058	**High D, High N**	1.34	1.7	6.31	-	15.39	8	5
33059		1.34	1.7	6.32	4	24	4	5
33475		1.4	1.67	6.16	5	24.4	5	7.5
33478		1.37	2.37	7	9.2	24.4	9.2	1.5

Figures

Figure 1

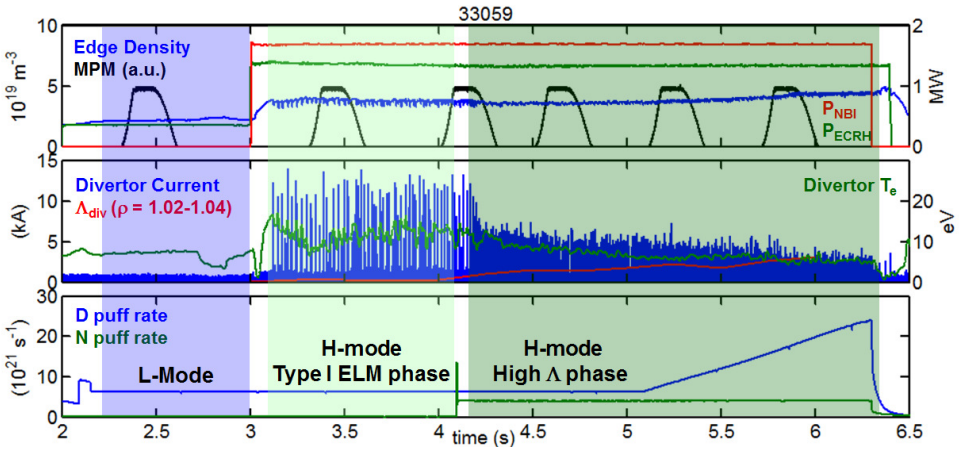

Figure 2

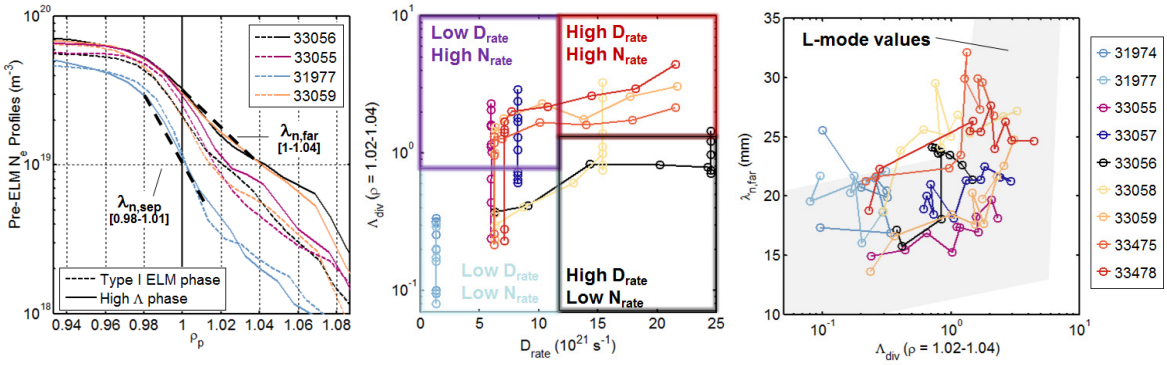

Figure 3

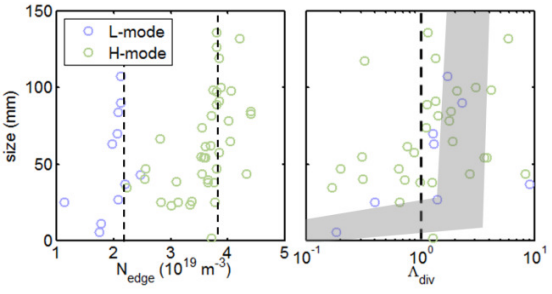

Figure 4

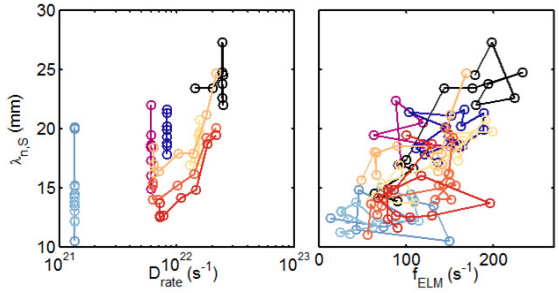

Figure 5